




# Reliable Index Modulation Aided Spatial $M$ -ary DCSK Design

Zuwei Chen<sup>1</sup>, Lin Zhang<sup>1</sup>(✉) , and Zhiqiang Wu<sup>2,3</sup>

<sup>1</sup> School of Electronics and Information Technology, Sun Yat-sen University, Guangzhou 510006, China

isszl@mail.sysu.edu.cn

<sup>2</sup> Department of Electrical Engineering, Tibet University, Lhasa 850012, China

<sup>3</sup> Department of Electrical Engineering, Wright State University, Dayton 45435, USA

**Abstract.** Higher order modulation and spatial modulation schemes improve the data rate for differential chaos shift keying (DCSK) systems by transmitting more bits in one time slot, however, the reliability performances become worse respectively due to more dense signal distributions and bad channel condition of active antenna. In this paper, we propose to utilize the antenna and symbol indexes to improve both the data rate and the reliability performances for DCSK systems with aid of antenna selection. Therein the information is modulated cooperatively using the antenna index and the symbol index. Then with the aid of the feedback channel state information (CSI) from receivers, the antenna with the best CSI is selected to transmit modulated symbols, which helps to improve the reliability performance. At the receiver, reverse operations are performed. Furthermore, we provide the theoretical symbol error rate (SER) and bit error rate (BER) over the multi-path Rayleigh fading channel. Simulation results demonstrate that the proposed scheme achieves better reliability performances than the counterpart schemes with the same data rate.

**Keywords:** Differential chaos shift keying (DCSK) · Index modulation · Multiple input multiple output (MIMO) · Spatial modulation (SM) · Reliability performances

## 1 Introduction

Differential chaos shift keying (DCSK) schemes have aroused a lot of research interests since no chaotic synchronization circuits are required at the receiver, which is attractive for practical implementations. Although DCSK systems inherit the benefits of chaotic communications including secure and robust transmissions, they sacrifice the data rate performances owing to the transmission of reference chaotic signals.

In order to achieve high data rate, higher modulation and spatial multiplexing have been utilized. Specifically, quadrature chaos shift keying [1] (QCSK) utilizes Hilbert transform to convey one more bits on one chaotic sequence. Then [2, 3] exploit the idea of a round constellation similar to phase shift keying (PSK) to further improve QCSK scheme to transmit more bits, and [4] utilizes orthogonal chaotic sequences to generate the QCSK-based  $M$ -ary DCSK signals based on a square constellation similar to the quadrature amplitude modulation (QAM). In addition, [5] uses  $M$ -order Walsh code (WC) to increase the data rate.

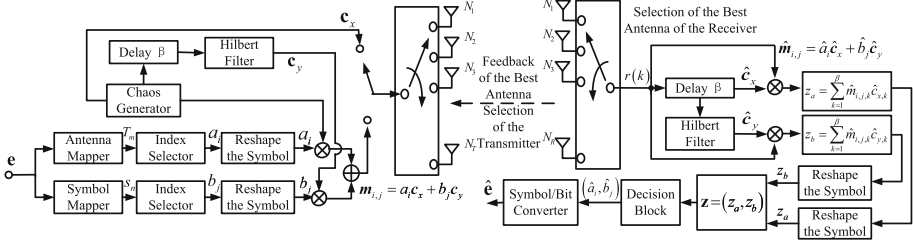
On the other hand, the spatial multiplexing provided by multiple input multiple output (MIMO) antennas is also exploited to improve the data rate. [6] presents a DCSK system using space-time coding based on Alamouti scheme, while [7] applies the orthogonal space-time block coding aided DCSK scheme. Moreover, [8] combines the high order modulation with the spatial multiplexing, and presents a MIMO  $M$ -ary DCSK scheme to be used when the channel state information (CSI) can hardly be obtained, and the spatial modulation (SM) is proposed in [9] to further improve the efficiency with a low complexity. However, due to more dense signal distributions and bad channel condition of active antenna, high order  $M$ -ary and SM aided DCSK systems may suffer from reliability performance degradations, especially when channel varies dramatically.

In order to achieve a better tradeoff between the reliability and data rate performances, in this paper, we propose to jointly utilize the antenna index and the symbol index to modulate the information, and present an index modulation-aided spatial  $M$ -ary DCSK (IM-S- $M$ -DCSK).

To be more explicit, at the transmitter, the input information is modulated and embedded into the symbol index and the antenna index jointly. Then the index modulated symbols are modulated by the reference chaotic sequence and its orthogonal version obtained from Hilbert transform to generate high order chaotic modulated symbols. The resultant modulated chaotic symbol is then transmitted via the antenna with the best CSI, which can be easily obtained from the receiver via the feedback channel. At the receiver, reverse operations are performed with a low complexity since only one signal received from the antenna with the best CSI is required to be processed.

Briefly, the main contributions include: (1) both the antenna index and the symbol index are exploited to modulate the same transmitted symbol and the feedback CSI is utilized to identify which antenna is selected to transmit chaotic modulated symbols; (2) the complexity of the receiver is reduced compared with other scheme adopting SM technology; (3) we provide the theoretical bit error rate (BER) and symbol error rate (SER) expressions over multi-path Rayleigh fading channels.

The remainder of the letter is organized as follows. The IM-S- $M$ -DCSK scheme is presented in Sect. 2, then in Sect. 3, we derive theoretical BER and SER expressions. Simulations and corresponding results are provided in Sect. 4. Finally, we conclude this paper in Sect. 5.


**Fig. 1.** IM-S- $M$ -DCSK transceiver.

**Table 1.** Mapping rule.

	Bits	Selected Antenna or Symbol	Select- ed Index	Reshape the Symbol		$m_{i,j} = \tilde{a}_i \mathbf{c}_x + \tilde{b}_j \mathbf{c}_y$
$N_T = 2, \tilde{M} = 2$	0	$T_1$	$s_1$	1	$-d$	$d \begin{bmatrix} -\mathbf{c}_x - \mathbf{c}_y & \mathbf{c}_x - \mathbf{c}_y \\ -\mathbf{c}_x + \mathbf{c}_y & \mathbf{c}_x + \mathbf{c}_y \end{bmatrix}$
$M = 4$	1	$T_2$	$s_2$	2	$d$	
$N_T = 4$	00	$T_1$	$s_1$	1	$-3d$	$d \begin{bmatrix} -3\mathbf{c}_x - 3\mathbf{c}_y & -3\mathbf{c}_x - \mathbf{c}_y & -3\mathbf{c}_x + \mathbf{c}_y & -3\mathbf{c}_x + 3\mathbf{c}_y \\ -\mathbf{c}_x - 3\mathbf{c}_y & -\mathbf{c}_x - \mathbf{c}_y & -\mathbf{c}_x + \mathbf{c}_y & -\mathbf{c}_x + 3\mathbf{c}_y \\ \mathbf{c}_x - 3\mathbf{c}_y & \mathbf{c}_x - \mathbf{c}_y & \mathbf{c}_x + \mathbf{c}_y & \mathbf{c}_x + 3\mathbf{c}_y \\ 3\mathbf{c}_x - 3\mathbf{c}_y & 3\mathbf{c}_x - \mathbf{c}_y & 3\mathbf{c}_x + \mathbf{c}_y & 3\mathbf{c}_x + 3\mathbf{c}_y \end{bmatrix}$
$\tilde{M} = 4$	01	$T_2$	$s_2$	2	$-d$	
	11	$T_3$	$s_3$	3	$d$	
$M = 16$	10	$T_4$	$s_4$	4	$3d$	

## 2 IM-S- $M$ -DCSK Scheme

### 2.1 Structure of the Scheme

In this section, we will elaborate the structure of the IM-S- $M$ -DCSK scheme. Figure 1 illustrates the transceiver structure of the proposed scheme.

At the transmitter, the input information is firstly modulated by the symbol index and the antenna index jointly. Then the signals bearing index modulated symbols are further modulated by orthogonal chaotic sequences alternately. Subsequently, the resultant chaotic modulated signals are transmitted through the channel with the best CSI selected from  $N_T \times N_R$  MIMO channels.

At the receiving end, after the transmission over independently and identically distributed (i.i.d.) fading channels, the receiver mounted with  $N_R$  antennas activate the specific selected antenna corresponding to the channel with the best CSI, and perform reverse operations to retrieve the information. More details about the IM-S- $M$ -DCSK design are given as below.

### 2.2 Transmitter

At the transmitter side, the chaos generator module outputs the chaotic sequences to modulate the symbols obtained from the index modulators to formulate the spatial  $M$ -DCSK signals for transmissions.

**Chaos Generator.** Here we adopt the second order Chebyshev polynomial function to generate the chaotic sequences of length  $\beta$ , which is expressed as

$$u_{v+1} = 1 - 2u_v^2 \quad (1)$$

where  $u_v$  denotes the  $v$ -th chip of the chaotic sequence. Based on Eq. (1), we use  $\mathbf{c}_x = (c_{x,1}, \dots, c_{x,\beta})$  to denote the first part of chaotic sequences output from the chaos generator, and  $c_{x,k}$  ( $k = 1, 2, \dots, \beta$ ) is the  $k$ th generated chip of the chaotic sequence.

Then we use Hilbert transform to generate another quadrature chaotic sequence, which is represented by  $\mathbf{c}_y = (c_{y,1}, \dots, c_{y,\beta})$  [1]. Thus, we have  $\sum_{k=1}^{\beta} c_{x,k} c_{y,k} = 0$ . Then the resultant chaotic sequence is normalized to achieve  $\sum_{k=1}^{\beta} c_{x,k}^2 = \sum_{k=1}^{\beta} c_{y,k}^2 = 1$ .

**Index Modulation-Aided Spatial  $M$ -DCSK.** As shown in Fig. 1, the input bit sequence  $\mathbf{e}$  is divided into two parts, the first  $\log_2(N_T)$  bits are mapped onto a selected antenna denoted by  $T_n$  ( $n = 1, \dots, N_T$ ), while another  $\log_2(\tilde{M})$  bits of the second part are mapped into a selected symbol denoted by  $S_m$  ( $m = 1, \dots, \tilde{M}$ ) where  $M = N_T \times \tilde{M}$ . Notably, the mapping rule from the bits to  $T_n$  and  $S_m$  follows the Gray decoding.

Subsequently, the subscripts  $n$  and  $m$  in  $T_n$  and  $S_m$  are transformed to the decimal number  $a_i$  ( $i = 1, \dots, N_T$ ) and  $b_j$  ( $j = 1, \dots, \tilde{M}$ ), which respectively correspond to the antenna index and the symbol index.

To be more explicit, as shown in Table 1, the index modulation is carried out by transforming the data bits to  $a_i$  and  $b_j$  by applying the Gray decoding. Then we reshape the indexes, i.e.,  $\tilde{a}_i = (2a_i - (N_T + 1))d$ ,  $\tilde{b}_j = (2b_j - (M + 1))d$ , which are used respectively as the  $x$ -axis coordinate and  $y$ -axis coordinate of a specific constellation point in the modulation constellation, where  $d$  denotes the unit distance between two constellation points in the constellation map.

After the index modulation, the resultant  $\tilde{a}_i$  and  $\tilde{b}_j$  are separately modulated by chaotic sequences  $\mathbf{c}_x$  or  $\mathbf{c}_y$ . The resultant chaotic modulated symbol is expressed as  $\mathbf{m}_{i,j} = \tilde{a}_i \mathbf{c}_x + \tilde{b}_j \mathbf{c}_y$ , which is transmitted during the  $q$ -th symbol duration via the antenna with the best channel gain as follows

$$s(k) = \begin{cases} c_{x,k}, & k = 2(q-1)\beta + 1, \dots, (2q-1)\beta \\ \tilde{a}_i c_{x,k} + \tilde{b}_j c_{y,k}, & k = (2q-1)\beta + 1, \dots, 2q\beta \end{cases} \quad (2)$$

Furthermore, Fig. 2 illustrates the constellation diagram. It can be seen that thanks to Gray decoding, each symbol has only one bit different from the neighbor constellation point and hence the received symbol intruding the neighbor point's decision area would cause only one bit error.

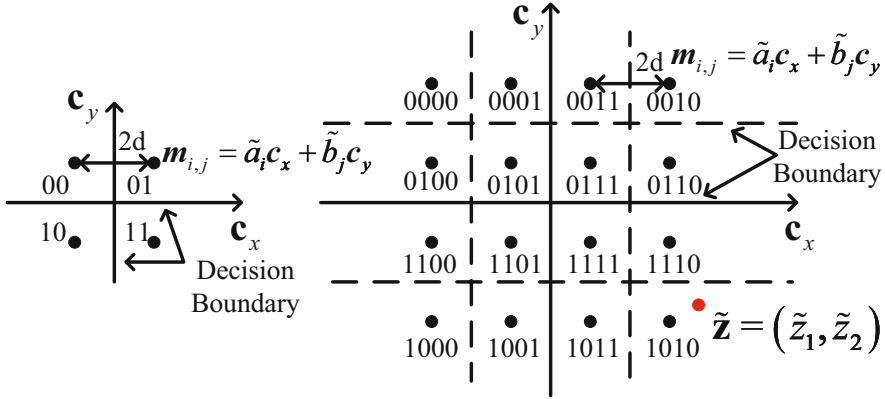


Fig. 2. Constellation diagram.

### 2.3 Receiver and Decision

As shown in Fig. 1, after the channel transmission, corresponding to the  $k_{th}$  chip in the  $q$ -th symbol duration, the received signal is obtained as

$$r(k) = h(k) \otimes s(k) + n(k) \tag{3}$$

where  $\otimes$  is the convolution operator, and  $n(k)$  is a wideband additive white Gaussian noise (AWGN) with zero mean and variance  $N_0/2$ . We consider a multipath slow Rayleigh fading channel, which is commonly used in spread spectrum systems [3, 4, 10], with the impulse response function of

$$h(k) = \sum_{l=1}^L \alpha_l \delta(k - \tau_l) \tag{4}$$

where  $L$  is the number of paths,  $\alpha_l$  and  $\tau_l$  are respectively the channel coefficient and the path time delay of the  $l$ -th path.

As shown in Fig. 1, corresponding to the two components of sequentially transmitted signals, the received signals can be easily separated into two parts. One is the first  $\beta$  chips denoted by  $\hat{c}_x$  and the other is the last  $\beta$  chips denoted by  $\hat{m}_{i,j} = \hat{a}_i \hat{c}_x + \hat{b}_j \hat{c}_y$  where  $\hat{c}_y$  is similarly obtained by performing Hilbert transform on  $\hat{c}_x$ .

Then the correlation demodulation is carried out respectively on the antenna index modulated symbols and the symbol index modulated symbols, and the corresponding decision variable are respectively determined by

$$z_a = \sum_{k=1}^{\beta} \hat{m}_{i,j,k} \hat{c}_{x,k} \quad z_b = \sum_{k=1}^{\beta} \hat{m}_{i,j,k} \hat{c}_{y,k} \tag{5}$$

where  $\hat{m}_{i,j,k}$  is the  $k$ -th chip of  $\hat{m}_{i,j}$ . Then, we reshape the decision variable and the resultant decision variables can be denoted by  $\tilde{z}_a = z_a / \sum_{l=1}^L \alpha_l^2$  and  $\tilde{z}_b = z_b / \sum_{l=1}^L \alpha_l^2$ .

Subsequently, demapping operations are performed based on Fig. 2, and the estimates of the user information, which is represented by  $\hat{\mathbf{e}}$ , can be obtained by evaluating the distance from a specific symbol to the constellation point. For example, as shown in Fig. 2, assuming that  $M = 16$  and the decision vector is  $\bar{\mathbf{z}} = (\bar{z}_1, \bar{z}_2)$ , we can naturally obtain the estimates as “1010” since  $\bar{\mathbf{z}} = (\bar{z}_1, \bar{z}_2)$  has the nearest distance with the point  $(3d, -3d)$ .

Next, based the above signal expressions, we will evaluate the theoretical error rate performances and derive SER and BER expressions.

### 3 Performance Analysis

In this section, we apply the Gaussian approximation method to derive the theoretical SER and BER expressions, which are dependent on the probability density distribution (PDF) of the channel with the best gain given as below.

#### 3.1 Probability Density Function Derivation

For  $L$  independent Rayleigh fading channels having the equal variances, the PDF of the symbol SNR  $\gamma_s$  is given by [11]

$$f_{\gamma_k}(\gamma_s) = \frac{\gamma_s^{L-1}}{(L-1)! \bar{\gamma}_p^L} \exp\left(-\frac{\gamma_s}{\bar{\gamma}_p}\right) \quad (6)$$

where  $\gamma_s$  is determined by  $\gamma_s = \left(\sum_{l=1}^L \alpha_l^2\right) \frac{E_s}{N_0}$ , where  $\sum_{l=1}^L \mathbb{E}[\alpha_l^2] = 1$ ,  $E_s$  is the average transmitted energy per symbol, and  $N_0$  is the variance of the complex AWGN, and  $\bar{\gamma}_p$  is the average symbol SNR per channel, which can be calculated by  $\bar{\gamma}_p = \left(\frac{E_s}{N_0}\right) \mathbb{E}[\alpha_l^2] = \left(\frac{E_s}{N_0}\right) \mathbb{E}[\alpha_o^2]$ ,  $l \neq o$ .

In addition, based on the properties of the chi-square distribution, the corresponding cumulative density function (CDF) is derived as

$$\Pr(\gamma_p \leq \gamma_s) = 1 - \exp\left(-\frac{\gamma_s}{\bar{\gamma}_p}\right) \sum_{k=0}^{L-1} \frac{1}{k!} \left(\frac{\gamma_s}{\bar{\gamma}_p}\right)^k \quad (7)$$

In our IM-S- $M$ -DCSK system, the PDF of the MIMO channel that is selected to transmit the signal with the best CSI is given as follows [12]

$$f_{\gamma_s}(\gamma_s) = \sum_{g=1}^{N_T \times N_R} f_{\gamma_g}(\gamma_s) \prod_{p=1, p \neq g}^{N_T \times N_R} \Pr(\gamma_p \leq \gamma_s) \quad (8)$$

#### 3.2 Theoretical SER Expression

Without loss of generalization, we assume that the largest multipath delay is much shorter than the symbol duration and the inter-symbol interference (ISI)

can be accordingly neglected. In addition, we also assume that the channel coefficient is constant during each symbol duration. Then we approximate the decision variables in Eq. (5) as approximated as

$$\begin{aligned}
 z_a &\approx \sum_{k=1}^{\beta} \left[ \left( \sum_{l=1}^L \alpha_l c_{x,k-\tau_l} + n_k \right) \right. \\
 &\quad \left. \times \left( \sum_{l=1}^L \alpha_l (a_i c_{x,k-\tau_l} + b_j c_{y,k-\tau_l}) + n_{k+\beta} \right) \right] \\
 z_b &\approx \sum_{k=1}^{\beta} \left[ \left( \sum_{l=1}^L \alpha_l c_{y,k-\tau_l} + n'_k \right) \right. \\
 &\quad \left. \times \left( \sum_{l=1}^L \alpha_l (a_i c_{x,k-\tau_l} + b_j c_{y,k-\tau_l}) + n_{k+\beta} \right) \right]
 \end{aligned} \tag{9}$$

where  $n_k$  is additive white Gaussian noise (AWGN) [1], and  $n'_k$  is obtained by performing Hilbert transform on  $n_k$ . Notably, when ideal Hilbert transform is performed,  $n'_k$  has the same statistics as  $n_k$ .

For large spreading factor, considering that the chaotic sequence has the property of  $\sum_{k=1}^{\beta} c_{x,k-\tau_l} c_{x,k-\tau_p} \approx 0$ ,  $l \neq p$  [10], Eq. (9) can be further simplified as

$$\begin{aligned}
 z_a &\approx \sum_{k=1}^{\beta} \sum_{l=1}^L \alpha_l (a_i c_{x,k-\tau_l} + b_j c_{y,k-\tau_l}) n_k + \sum_{k=1}^{\beta} n_k n_{k+\beta} \\
 &\quad + \sum_{l=1}^L a_i \alpha_l^2 \sum_{k=1}^{\beta} c_{x,k-\tau_l}^2 + \sum_{k=1}^{\beta} \sum_{l=1}^L \alpha_l c_{x,k-\tau_l} n_{k+\beta} \\
 z_b &\approx \sum_{k=1}^{\beta} \sum_{l=1}^L \alpha_l (a_i c_{x,k-\tau_l} + b_j c_{y,k-\tau_l}) n'_k + \sum_{k=1}^{\beta} n'_k n_{k+\beta} \\
 &\quad + \sum_{l=1}^L b_j \alpha_l^2 \sum_{k=1}^{\beta} c_{x,k-\tau_l}^2 + \sum_{k=1}^{\beta} \sum_{l=1}^L \alpha_l c_{y,k-\tau_l} n_{k+\beta}
 \end{aligned} \tag{10}$$

Recall that in  $M$ -order square constellation,  $\tilde{M} = N_T = \sqrt{M}$ , and the amplitudes of constellation points are respectively  $\pm d, \dots, \pm (\sqrt{M} - 1) d$ , the energy of a specific symbol determined by

$$\begin{aligned}
 E_s &= \frac{1}{M} \sum_{i=1}^{N_T} \sum_{j=1}^{\tilde{M}} (a_i^2 + b_j^2 + 1) \sum_{k=1}^{\beta} c_x^2 = \text{E} (a_i^2 + b_j^2 + 1) \\
 &= \frac{2(M-1)d^2 + 3}{3}
 \end{aligned} \tag{11}$$

Then we can derive the mean and the variance of decision variables as

$$\begin{aligned}
 \mathbb{E}[z_a] &= a_i \sum_{l=1}^L \alpha_l^2 & \mathbb{E}[z_b] &= b_j \sum_{l=1}^L \alpha_l^2 \\
 \text{var}[z_a] &= \sum_{l=1}^L \alpha_l^2 \mathbb{E}[a_i^2 + b_j^2 + 1] \frac{N_0}{2} + \frac{\beta N_0^2}{4} \\
 &\approx \sum_{l=1}^L \alpha_l^2 \frac{E_s N_0}{2} + \frac{\beta N_0^2}{4} \\
 \text{var}[z_b] &\approx \sum_{l=1}^L \alpha_l^2 \frac{E_s N_0}{2} + \frac{\beta N_0^2}{4}
 \end{aligned} \tag{12}$$

For transmissions over AWGN channel, based on Eq. (12), we can be derive that both decision variables have the variance of  $\frac{E_s N_0}{2} + \frac{\beta N_0^2}{4}$  before and after reshaping. Thus the conditional probability that the decision variable  $\tilde{z}$  exceeds the boundaries in the constellation map is determined by

$$P_e = \Pr(|\tilde{z}_a - a_i| > d) = 2Q\left(\frac{d}{\sqrt{\frac{E_s N_0}{2} + \frac{\beta N_0^2}{4}}}\right) \tag{13}$$

Accordingly, we can derive the SER expression based Eqs. (11) and (13) as

$$\begin{aligned}
 P_s^{AWGN}(\gamma_s) &= 1 - \left[1 - \frac{\sqrt{M}-1}{\sqrt{M}} P_e\right]^2 \\
 &= 1 - \left[1 - \frac{2(\sqrt{M}-1)}{\sqrt{M}} Q\left(\frac{6d\gamma_s / (2(M-1)d^2 + 3)}{\sqrt{2\gamma_s + \beta}}\right)\right]^2
 \end{aligned} \tag{14}$$

where  $Q(x) = 1/\sqrt{2\pi} \times \int_x^\infty \exp(-t^2/2) dt$ , for  $x \geq 0$ .

When transmitted over slow and flat Rayleigh fading channels, the SER expression is expressed as

$$P_s^{Rayleigh} = \int_0^{+\infty} P_s^{AWGN}(\gamma_s) f(\gamma_s) d\gamma_s \tag{15}$$

where  $f(\gamma_s)$  is given by Eq. (8).

### 3.3 Theoretical BER Calculation

Based on Eq. (14), by referring to [13], we can get the BER expression over the AWGN channel as

$$P_b^{AWGN}(\gamma_s) = \frac{\sum_{p=1}^{\log_2 \sqrt{M}} \sum_{w=0}^W T_w^p \operatorname{erfc}\left(\frac{F_w \gamma_s}{\sqrt{2\gamma_s + \beta}}\right)}{\sqrt{M} \log_2 \sqrt{M}} \tag{16}$$



where  $T_w^p = (-1)^{\lfloor \frac{w \times 2^{p-1}}{\sqrt{M}} \rfloor} \left( 2^{p-1} - \left\lfloor \frac{w \times 2^{p-1}}{\sqrt{M}} + \frac{1}{2} \right\rfloor \right)$ ,  $W = (1 - 2^{-p})\sqrt{M} - 1$ , and  $F_w = \frac{6(2w+1)d}{\sqrt{2(2(M-1)d^2+3)}}$ , where  $\lfloor x \rfloor$  denotes the largest integer of  $x$ , and  $\text{erfc}(x) = 2/\sqrt{\pi} \times \int_x^\infty \exp(-t^2) dt$ .

Then similar to Eq. (15), the BER expression over Rayleigh fading channels can be obtained as

$$P_b^{Rayleigh} = \int_0^{+\infty} P_b(\gamma_s) f(\gamma_s) d\gamma_s. \tag{17}$$

### 4 Simulation Results

In this section, we provide simulation results to verify the effectiveness of the theoretical analysis and to demonstrate the outstanding performances of our design under different parameter settings. In the simulations,  $d = \sqrt{3/(2(M-1))}$ , and we assume that perfect CSI and the same channel parameters are shared between the pair of transceivers.

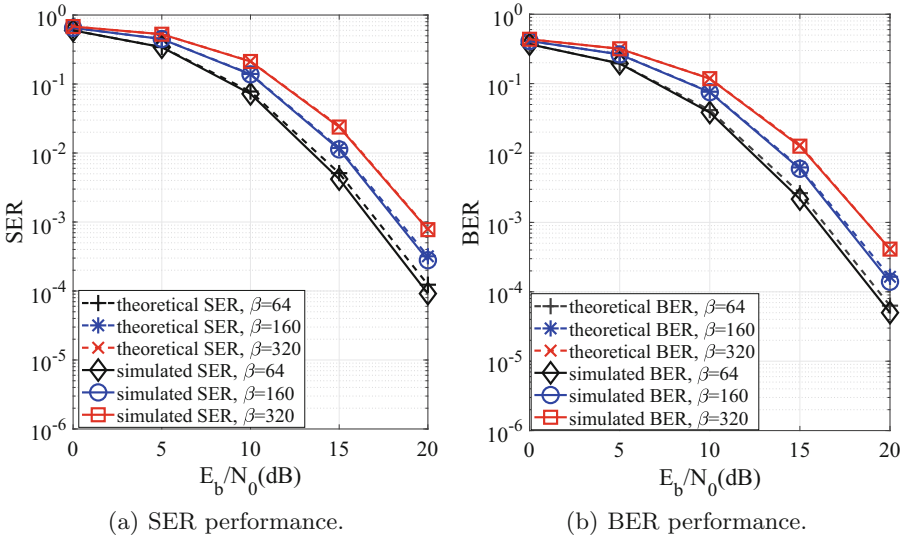


**Fig. 3.** Theoretical and simulated SER and BER performance comparisons over the single-path Rayleigh fading channel.  $N_T = 2$ ,  $N_R = 2$ ,  $\bar{M} = 2$ ,  $M = 4$ .

Firstly, Fig. 3(a) compares the theoretical SER and BER over the single-path Rayleigh fading channel when  $\beta = 64, 160, 320$ . It can be observed from Fig. 3(a) and (b) that for larger  $\beta$  such as  $\beta = 320$ , the theoretical SER and BER approximately overlap with the simulated ones, and are more consistent with the simulation results thanks to higher Gaussian approximation precision with more

samples than the case that  $\beta = 64$  and  $\beta = 160$ . Moreover, it is noticeable that for smaller  $\beta$ , the SER and BER performances are better than those with larger  $\beta$  since the interferences may increase when the value of  $\beta$  increases [4].

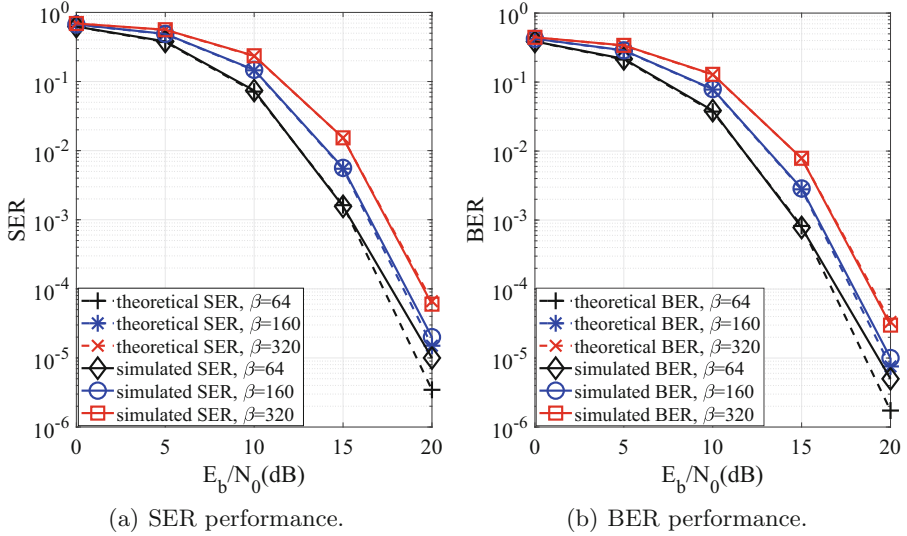


**Fig. 4.** Theoretical and simulated SER and BER performance comparisons over the 2-path Rayleigh fading channel.  $N_T = 2$ ,  $N_R = 2$ ,  $M = 2$ ,  $M = 4$ .

Subsequently, Fig. 4 verifies the effectiveness of theoretical SER and BER expressions over 2-path Rayleigh fading channels with  $E[\alpha_1^2] = E[\alpha_2^2] = 1/2$ ,  $\tau_1 = 0$ ,  $\tau_2 = 1$ . Similar to Fig. 3(a), we can observe that the theoretical results match the simulated ones not well for small  $\beta$ , and the reliability performances degrade with the increasing  $\beta$ .

Figure 5(a) and (b) respectively compare the presented IM-S- $M$ -DCSK scheme with the benchmark spatial modulation DCSK (SM-DCSK) scheme [9] when  $\beta = 64$ , and another benchmark square-constellation-based  $M$ -ary DCSK (S- $M$ -DCSK) [4] over a 2-path Rayleigh fading channel under different configuration parameters of antennas. The channel parameters are assumed as  $E[\alpha_1^2] = E[\alpha_2^2] = 1/2$ ,  $\tau_1 = 0$  and  $\tau_2 = 1$ . It can be seen from Fig. 5(a) and (b) that our IM-S- $M$ -DCSK systems achieve better reliability performances than benchmark schemes while providing higher data rate transmissions with higher order modulations. Moreover, for different  $N_T$  and  $N_R$ , IM-S- $M$ -DCSK MIMO systems can achieve better reliability performances than those of the single input single out (SISO) S- $M$ -DCSK systems [4]. In the Fig. 5(a), there is a performance lower bound for  $M = 16$  case because the inter-path interference cannot be ignored for the modulation order  $M = 16$  leading to a closer distance between symbols and a small spreading factor  $\beta = 64$  leading to a larger correlation value of signals over different paths. When  $\beta$  is enough large, the interpath

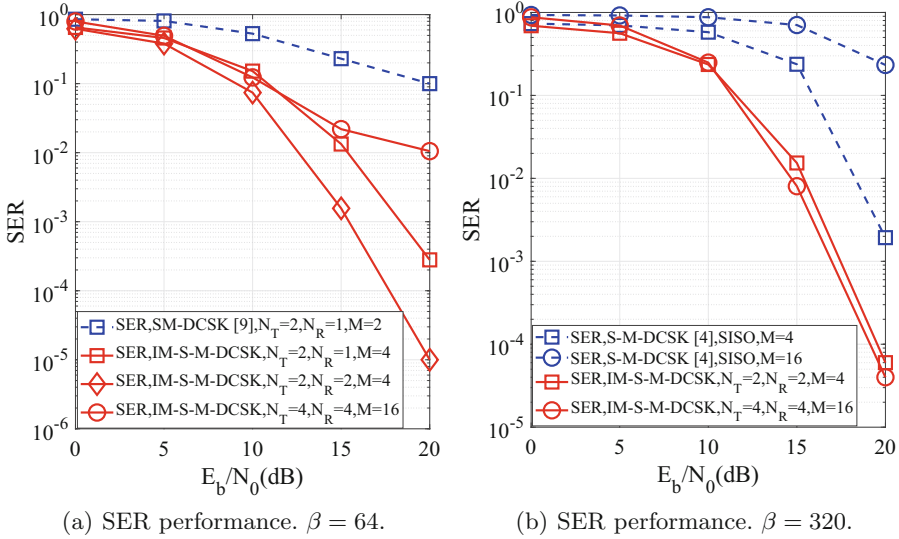


**Fig. 5.** SER performance comparisons with the SM-DCSK scheme [9] and S-M-DCSK [4] over the multipath Rayleigh fading channel.

interference is also able to be ignored for high modulation order just as  $M = 16$  case in Fig. 5(b).

### 5 Conclusion

In this paper, we address the issue of reliability performance degradation for high order or spatial modulation DCSK systems. In our design, we propose to use the antenna index and the symbol index modulating the symbol to ensure the data rate. The resultant chaotic modulated symbols are then transmitted over the channel with the best channel gain to eliminate the bad effect of the channel assignment for the traditional SM scheme and obtain well channel condition. Then we derive theoretical SER and BER expressions which have been verified via the performance comparisons with the simulation results. More over, the simulation results over fading channels under different parameter settings demonstrate that the presented IM-S-M-DCSK scheme achieves better reliability performances than the benchmark schemes while providing higher data rate transmissions. Last but not the least, it's worth pointing out that the presented index modulation aided design can be easily integrated with the MIMO-DCSK system and its low-complexity receiver and the high security of chaos signal is suitable for the devices in the Internet of things (IoT).

**Acknowledgements.** This work was supported by the National Natural Science Foundation of China (Grant No. 61602531) and State's Key Project of Research and Development Plan under (Grant 2017YFE0121300-6).

## References

1. Galias, Z., Maggio, G.M.: Quadrature chaos-shift keying: theory and performance analysis. *IEEE Trans. Circuits Syst. I Fundam. Theory Appl.* **48**(12), 1510–1519 (2001)
2. Cai, G., Fang, Y., Han, G.: Design of an adaptive multiresolution  $M$ -ary DCSK system. *IEEE Commun. Lett.* **21**(1), 60–63 (2017)
3. Wang, L., Cai, G., Chen, G.R.: Design and performance analysis of a new multiresolution  $M$ -ary differential chaos shift keying communication system. *IEEE Trans. Wireless Commun.* **14**(9), 5197–5208 (2015)
4. Cai, G., Fang, Y., Han, G., Lau, F.C.M., Wang, L.: A square-constellation-based  $M$ -ary DCSK communication system. *IEEE Access* **4**, 6295–6303 (2016)
5. Kolumbán, G., Kis, G.: Reception of  $M$ -ary FM-DCSK signals by energy detector. In: *Proceedings of the NDES 2003*, Scuol, Switzerland, pp. 133–136 (2003)
6. Kaddoum, G., Vu, M., Gagnon, F.: Performance analysis of differential chaotic shift keying communications in MIMO systems. In: *2011 IEEE International Symposium of Circuits and Systems (ISCAS)*, Rio de Janeiro, Brazil, pp. 1580–1583. IEEE (2011)
7. Wang, S., Lu, S., Zhang, E.: MIMO-DCSK communication scheme and its performance analysis over multipath fading channels. *J. Syst. Eng. Electron.* **24**(5), 729–733 (2013)
8. Wang, S., Wang, X.:  $M$ -DCSK-based chaotic communications in MIMO multipath channels with no channel state information. *IEEE Trans. Circuits Syst. II Exp. Briefs* **57**(12), 1001–1005 (2010)
9. Kumar, A., Sahu, P.R.: Performance analysis of spatially modulated differential chaos shift keying modulation. *IET Commun.* **11**(6), 905–909 (2017)
10. Xia, Y., Tse, C.K., Lau, F.C.M.: Performance of differential chaos-shift-keying digital communication systems over a multipath fading channel with delay spread. *IEEE Trans. Circuits Syst. II Exp. Briefs* **51**(12), 680–684 (2004)
11. Proakis, J.G., Salehi, M.: *Digital Communications*, 5th edn. McGraw-Hill, New York (2007)
12. Aydin, E., Ilhan, H.: A novel SM-based MIMO system with index modulation. *IEEE Commun. Lett.* **20**(2), 244–247 (2016)
13. Cho, K., Yoon, D.: On the general BER expression of one- and two-dimensional amplitude modulations. *IEEE Trans. Commun.* **50**(7), 1074–1080 (2002)